

Molecular Dynamics Simulations of Folding of Supported Graphene

Edson P. Bellido^{†,‡} and Jorge M. Seminario^{*,†,‡,§}

Department of Chemical Engineering, Materials Science and Engineering Graduate Program, Department of Electrical and Computer Engineering, Texas A&M University, College Station, Texas 77843, United States

Received: September 6, 2010; Revised Manuscript Received: November 2, 2010

The controlled folding of graphene structures driven by molecular interactions with water nanodroplets is analyzed taking into account interactions with supported substrates such as silicon dioxide (SiO_2), hexamethyldisilazane (HMDS), and isopropyl alcohol (IPA) on SiO_2 . The interaction between unsupported graphene and a water nanodroplet is strong enough to induce folding on graphene nanostructures. However, when the graphene is supported on SiO_2 , the attraction between graphene and the substrate prevents graphene from folding but if the substrate is a hydrophobic surface such as HMDS or a solvent such as IPA, the interaction between graphene and the substrate is weak, and depending on the geometry of the graphene structure, folding is possible. The selection of an acceptable substrate and graphene geometry opens the possibility of a controlled fabrication of graphene-based capsules, scrolls, sandwiches, and rings able to carry a payload.

Introduction

Since the discovery of carbon nanotubes in 1991,¹ carbon-based materials have been intensively investigated due to their unique mechanical and electrical properties,^{2–8} which make carbon materials ideal building blocks for future applications in areas as diverse as defense, electronics, energy, and medicine^{9–14} among others. Recently, a wrapped graphene sheet with a tubular structure (nanoscroll) was fabricated from single graphene sheets with the aid of a solution of isopropyl alcohol (IPA) and water.¹⁵ Similarly, other types of carbon nanostructures, such as capsules, sandwiches, and rings, are expected to acquire some of the properties of both graphene and carbon nanotubes.^{15,16} Patra et al. suggested a method to precisely control the fabrication of such carbon nanostructures using water nanodroplets.¹⁷ The method relies on the capability of the water cluster to cross the potential barrier of graphene deformation. However, when we consider a graphene sheet on a substrate, the graphene–substrate interaction increases the potential barrier that needs to be overcome by the Coulombic and/or van der Waals forces between the graphene and the nanodroplet.

In this work, we theoretically analyze the interaction between a nanodroplet and graphene structures supported on substrates such as silicon dioxide (SiO_2), isopropyl alcohol (IPA) on SiO_2 , and a film of hexamethyldisilazane (HMDS) on SiO_2 .

Methods

We perform molecular dynamics (MD) simulations with the LAMMPS¹⁸ program. The atomic interaction is modeled with the CHARMM¹⁹ force field. For the nonbonded interactions we consider Lennard–Jones potential,

* To whom correspondence should be addressed. E-mail: seminario@tamu.edu.

[†] Department of Chemical Engineering.

[‡] Materials Science and Engineering Graduate Program.

[§] Department of Electrical and Computer Engineering.

$$V_{\text{LJ}}(r_{ij}) = 4\varepsilon_{ij} \left[\left(\frac{\sigma_{ij}}{r_{ij}} \right)^{12} - \left(\frac{\sigma_{ij}}{r_{ij}} \right)^6 \right] \quad (1)$$

where $\varepsilon_{ij} = \sqrt{\varepsilon_i \varepsilon_j}$ is the minimum value of potential energy and is defined for each pair of atoms, and $\sigma_{ij} = (1/2)(\sigma_i + \sigma_j)$, are defined as the zero-crossing distances for the potential. Also Coulombic interactions are considered in the calculations,

$$C(r_{ij}) = \frac{cq_i q_j}{r_{ij}} \quad (2)$$

where q_i is the charge of each atom and $C = 1/4\pi\epsilon = 1.44 \times 10^{-9} \text{ V m e}^{-1}$ is the Coulomb constant and ϵ is the permittivity of vacuum. The nonbonded potentials are affected by a switching function:

$$S(r_{ij}) = \frac{[r_{\text{out}}^2 - r_{ij}^2]^2[r_{\text{out}}^2 + 2r_{ij}^2 - 3r_{\text{in}}^2]}{[r_{\text{out}}^2 - r_{\text{in}}^2]^3} \quad (3)$$

This function ramps the energy and force smoothly to zero between an inner (r_{in}) and outer (r_{out}) cutoff. When $r < r_{\text{in}}$, Lennard–Jones and Coulombic potentials are not affected by the switching function, and when $r_{\text{in}} < r < r_{\text{out}}$ all components are affected by the switching function $S(r_{ij})$.

The force field parameters for the molecular structures are adapted from previous works,^{17,20–25} the Lennard–Jones parameters are shown in Table 1 and the partial charges are shown in Figure 1. The charges for the graphene structures and for the SiO_2 substrate are calculated by molecular mechanics simulations using MMFF94s force field in Spartan'08, for IPA and HMDS the charges are calculated by ab initio calculations using B3PW91 hybrid functional^{26,27} and 6-31G(*d*) basis sets,²⁸ and for water we use the TIP3 model.

For HMDS, the harmonic parameters for bonds and angles are calculated using the program FUERZA,^{23–25} which is a procedure that takes the Hessian tensor from ab initio calcula-

TABLE 1: Lennard-Jones Parameters Used to Simulate the SiO₂ Substrate, Graphene Structures, Film of HMDS, Water Nanodroplet, and IPA^a

model	atom type	ϵ (kcal/mol)	σ (Å)
SiO ₂	O	-0.152	3.154
	Si	-0.300	3.826
graphene	C	-0.070	3.550
	N	-0.200	3.296
HMDS	H-N	-0.022	2.352
	Si	-0.300	3.409
H ₂ O	C	-0.110	3.564
	H	-0.022	2.352
IPA	O	-0.152	3.151
	H	-0.046	0.400
	C	-0.020	4.054
	H	-0.022	2.352
	O	-0.152	3.154
	H-O	-0.046	0.400

^a For HMDS the atom type called H-N represents the hydrogen atom bonded to the nitrogen atom (Figure 1d) and for IPA the atom type called H-O represents the hydrogen bonded to the oxygen atom (Figure 1b).

tions to calculate the force field parameters. Table 2 shows the bond parameter and Table 3 shows the angle parameters.

The input files of the model structures are constructed using Spartan'08, Packmol,²⁹ Ampac GUI 9, and homemade software. A 6 × 6 nm flower like structure is constructed with two of the

TABLE 2: Bond Harmonic Parameters Used to Simulate HMDS

bond type	force constant (kcal/mol)	bond distance (Å)
H-C	356.28	1.0967
C-Si	169.90	1.8893
Si-N	226.62	1.7517
H-N	493.17	1.0156

TABLE 3: Angle Harmonic Parameters Used to Simulate HMDS

angle type	force constant (kcal/mol)	angle (degrees)
H-C-H	-44.08	107.6
Si-C-H	-55.29	111.3
C-Si-C	-121.23	109.1
N-Si-C	-122.99	109.8
Si-N-Si	-134.75	133.7
H-N-Si	-42.23	113.0

petals with zigzag edges and two with armchair edges, and a nanodroplet (140 water molecules) positioned at the middle of the graphene structure (Figures 2 and 3). Also a flake structure is constructed with two flakes of 3 × 2 nm connected by a bridge of 2 × 0.7 nm, a nanodroplet with 472 water molecules is positioned over the bridge (Figure 4a). The SiO₂ structure has dimensions of 8 × 8 × 1 nm³. During the simulations, the base of the SiO₂ is fixed to simulate the bulk structure. The simulations are carried out with a time step of 1 fs and inner

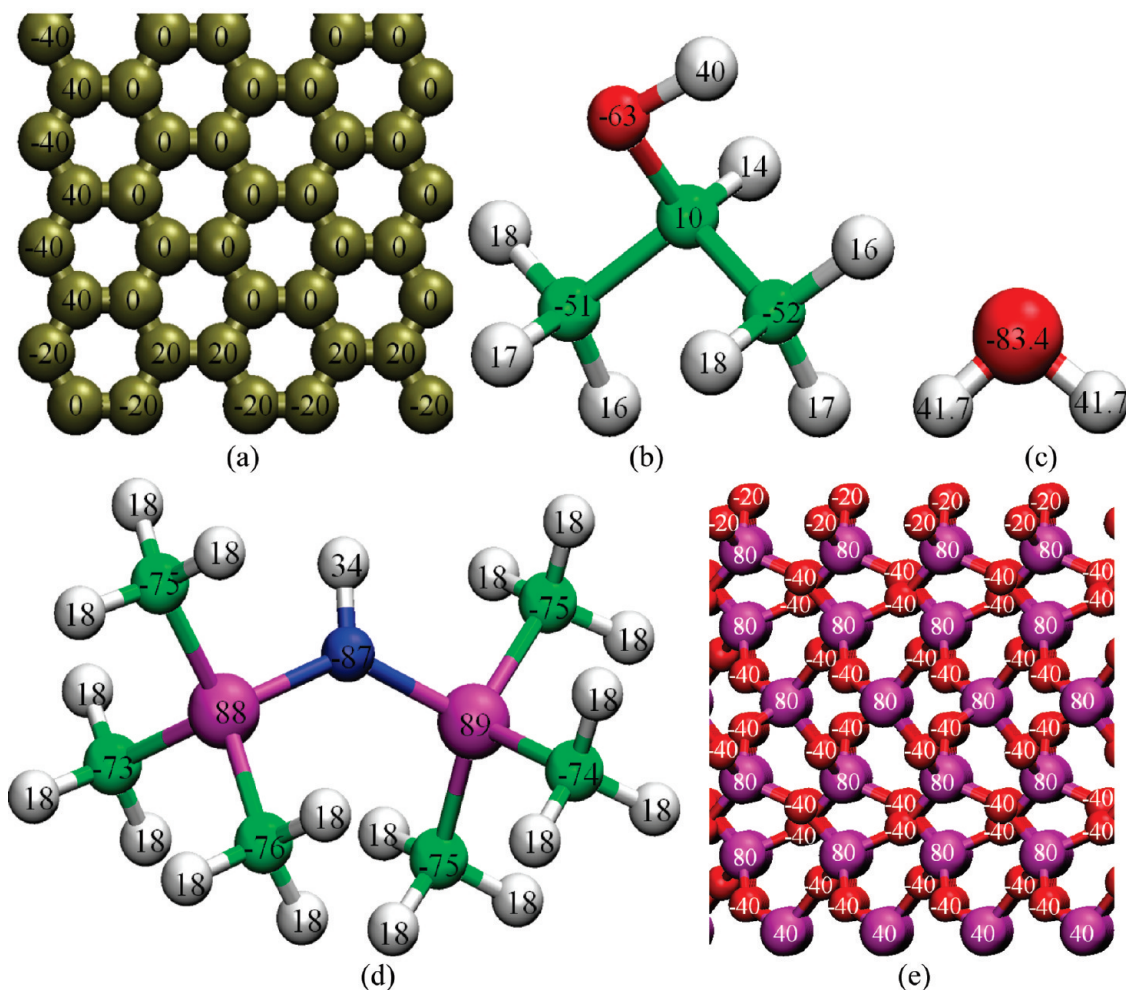


Figure 1. Partial charges of (a) graphene structures, (b) IPA, (c) water, (d) HMDS, and (e) SiO₂. All charges are in e/100 units, the atoms are color coded: graphene C (tan), IPA and HMDS C (green), H (white), O (red), N (blue), and Si (magenta).

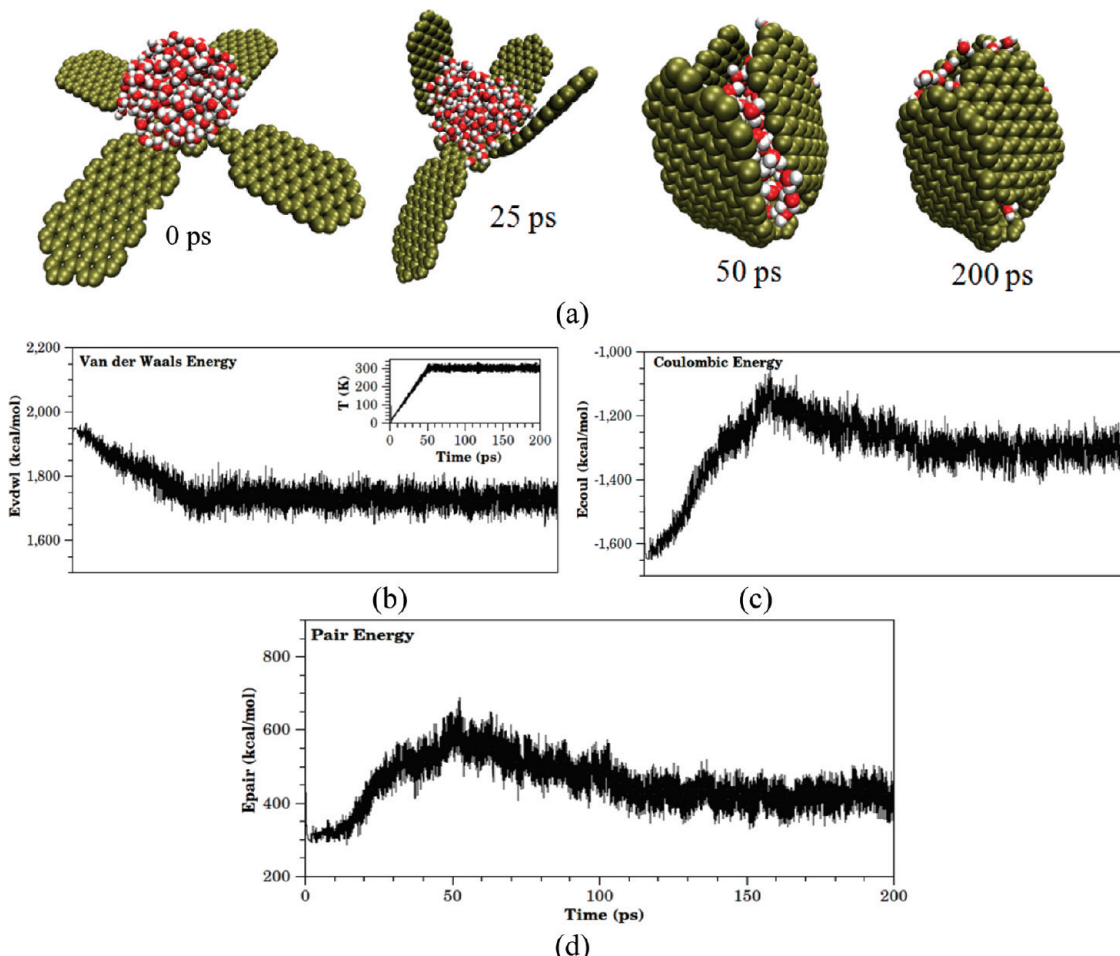


Figure 2. (a) Snapshots of the dynamics of the folding process driven by interactions between the graphene and nanodroplet at 0, 25, 50, and 200 ps, and time evolutions of the (b) van der Waals energy, (c) Coulombic energy, and (d) pair energy during the molecular dynamics simulation.

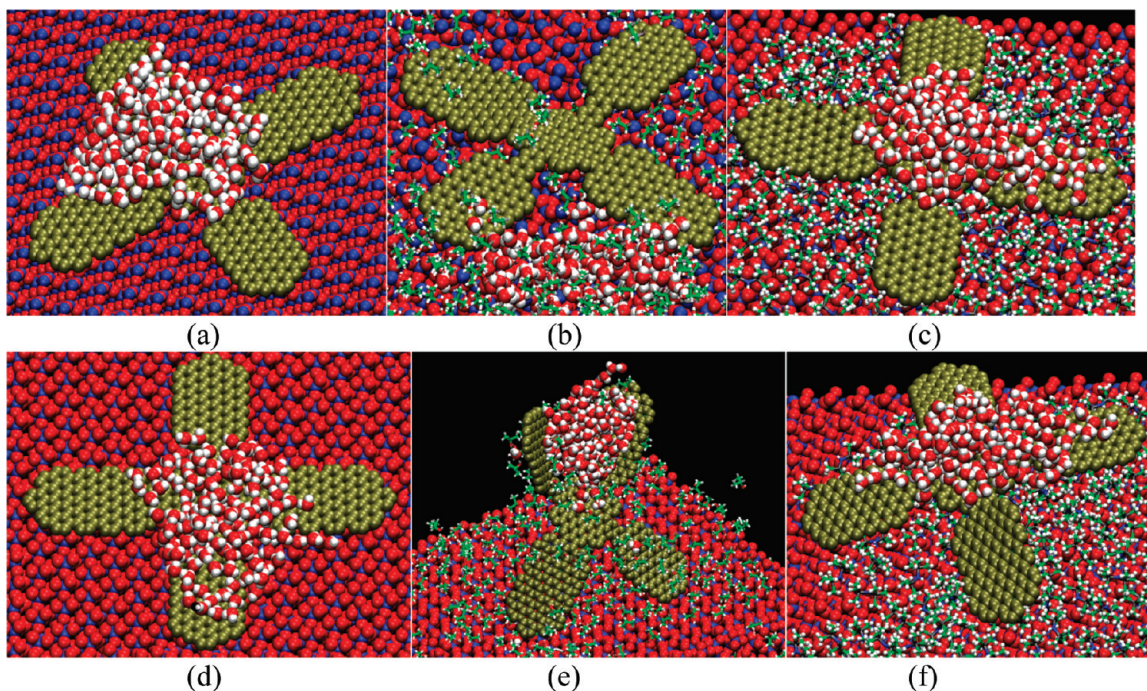


Figure 3. Interaction of a graphene flower structure with (a) a nanodroplet on SiO₂, (b) on IPA layer SiO₂ supported, and (c) on a HMDS layer SiO₂ supported. Interaction of the defective flower system with (d) SiO₂, (e) IPA layer supported on SiO₂, and (f) HMDS layer supported on SiO₂.

and outer cutoffs of 60 and 65 Å, respectively. After a minimization, the simulations follow a ramp of temperature with

a Nose–Hoover thermostat³⁰ from 10 to 300 K and a damping time of 100 fs. Then, the systems are kept at 300 K with the

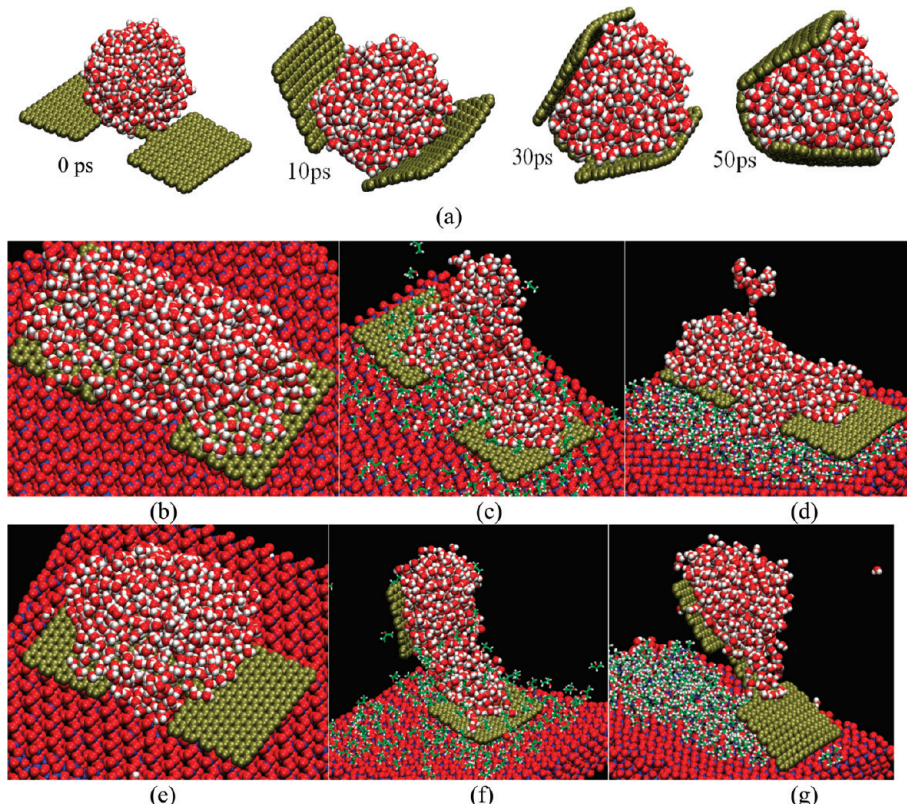


Figure 4. (a) Folding dynamics of the graphene flake structure. Interaction of a graphene flake structure with (b) a water nanodroplet on SiO_2 , (c) an IPA layer supported on SiO_2 , and (d) an HMDS layer supported on SiO_2 . Interaction of the defective flake system with (e) SiO_2 , (f) IPA layer supported on SiO_2 , and (g) HMDS layer supported on SiO_2 .

same damping time, until the systems reach equilibrium. For the flower-like structure, ab initio calculations are also performed to get the binding energy of the system; the method and basis set used are Hartree–Fock and 3-21G, respectively.

Results

We study first the interaction of the flower like graphene structure and a water nanodroplet when the system is isolated and no-substrate interaction is considered (Figure 2). The system is heated to 300 K, during the heating steps the structure vibrates and begins to get closer to the nanodroplet. At 25 ps, three of the four petals are partially closed, and finally at 50 ps, when the temperature reaches the 300 K, the petals are completely closed forming a nanocapsule with the water molecules inside. From 50 to 200 ps, the temperature is kept constant at 300 K and the nanocapsule is further stabilized; some water molecules are squeezed away.

To analyze the process of folding, we analyze the nonbonded interactions between the atoms of the graphene–nanodroplet system. During the heating steps (Figure 2), when the folding process is carried out, the van der Waals energy decreases; this occurs because the process of the closing of petals of the flower-like structure is driven by van der Waals attraction between the carbon atoms of the graphene and the water molecules; therefore, as the petals get closer to the nanodroplet, the van der Waals energy decreases until all the petals are closed. Between 50 and 200 ps, the petals of the nanostructure remain closed; therefore, the van der Waals energy also remains constant and the Coulombic energy increases between 0 to 50 ps; this is because when the petals get closer to the water molecules, the water molecules have less room to move and the Coulombic repulsion increases. However, between 50 to 200 ps, after the nanodroplet

is completely inside the graphene structure, some water molecules reaccommodate inside and others get away of the structure. This translates in a decrease of the Coulombic energy.

The pair energy is defined as the energy of nonbonded interactions, which in our case is the sum of van der Waals energy and Coulombic energy. Despite the fact that the pair energy increases during the closing of petals of the graphene structure, the energy drops as the nanocapsule is stabilized (Figure 2). To confirm our results, we perform ab initio calculations of the initial structure as shown in Figure 2a and of the completely closed structure. We find out that the binding energy of the initial structure and the completely folded graphene with the nanodroplet inside are -35.9 and -218.2 kcal/mol, respectively. These results suggest that the folding of the graphene structure is driven by a decrease in the graphene–nanodroplet binding energy and confirm that the process is energetically favorable.

When we analyze the graphene flower-like nanodroplet system supported on SiO_2 , using the same simulation parameters as in the case of the unsupported structure, the interaction between the graphene and the substrate does not allow the folding process to occur as shown in Figure 3a. There are three main factors that prevent the folding: first factor, the nonbonded interaction between the graphene nanostructure and the substrate is stronger than the interaction between graphene and water molecules; the second factor is that SiO_2 is more hydrophilic than graphene and for this reason the water nanodroplet expands trying to cover the SiO_2 surface preventing the graphene from folding; and the third factor is that depending on the geometry of the graphene and the water nanodroplet, the contact area between graphene and the substrate is larger than the contact area between graphene and the water nanodroplet.

In order to reduce the SiO_2 –graphene interaction, a system with a layer of IPA on top of SiO_2 is used as substrate; the results are similar as the case without IPA (Figure 3b). The contact area between the graphene flower and the substrate is larger compared to the graphene–nanodroplet contact area preventing the folding. To reduce the attraction between the water nanodroplet and the SiO_2 substrate, a hydrophobic layer of HMDS on top of SiO_2 is also tested; however, as in the previous cases, the folding does not occur (Figure 3c).

We simulated systems, in which we changed the initial geometry and position the graphene–nanodroplet structure 5 Å away from the substrate (defined as a defective system). This geometry is in agreement with experimental measurements where supported graphene sheets present corrugations with a height depending on the substrate, highs vary from 2 to 10 Å,^{31–33} also substrate surfaces were not completely flat and showed defects in the order of tens of nanometers.³⁴ We simulated the defective system supported on an IPA layer on top of SiO_2 ; since the IPA molecules screen the strong interaction between graphene and SiO_2 and since the initial geometry of the system have reduced the initial contact area between graphene and IPA, the interaction between the water molecules and graphene is not weakened, allowing the graphene folding process as seen in Figure 3e. This result is in agreement with Xie et al. experimental results;¹⁵ they fabricated nanoscrolls using a solution of water and IPA and the initial bending separating graphene from the surface was attributed to surface tension. Finally, we simulate the defective system supported on a layer of HMDS on SiO_2 ; in this case, the folding is initiated, however the interaction between graphene and HMDS is stronger compared to the water–graphene interaction and the folding does not occur (Figure 3f).

We also study a flake–nanodroplet system where the flake structure is simulated with the same simulation parameters as the flower structure; the main differences between both structures are that the flake structure has a larger area to interact with its environment and that the water nanodroplet in the flake system is larger than that in the flower system. The first test is the folding of the unsupported flake system (Figure 4a), where the folding is completed in a shorter time compared to the flower structure, which takes place at 25 ps, during the heating steps. The structure is completely folded and stabilizes further during the next heating steps and also when the temperature is kept at 300 K. The next tests are the simulations of the supported structure on SiO_2 , on a layer of IPA supported on SiO_2 , and on a layer of HMDS supported on SiO_2 ; as in the case of the flower-like structure, when the initial geometry is in close contact with the substrate, the folding does not occur (Figure 4b–d). This result is expected because the large surface area of the flake structure interacts strongly with the substrate surface and the van der Waals interaction with the water nanodroplet cannot overcome the substrate attraction.

We also perform simulations of the flake–nanodroplet structure positioned 5 Å away from the substrate as in the case of the flower structure for all of the previous analyzed substrates. When the defective system is supported on SiO_2 , despite the fact that the folding of the flake structure occurs in a shorter time than that in the flower system, the interaction with the SiO_2 surface is stronger and does not allow the folding as shown (Figure 4e). For the defective system supported on a layer of IPA on SiO_2 , as in the case of the flower-like structure, the folding process occurs (Figure 4f). Finally, in the defective system supported on a layer of HMDS on SiO_2 , the strong van der Waals interaction between the water nanodroplet and the

large surface area of the graphene flake overcomes the interaction between graphene and HMDS, allowing the graphene to fold. The character hydrophobic of the HMDS does not allow the water nanodroplet to lose the droplet structure favoring the folding process. This last test shows the importance of selecting the adequate geometry of the graphene structure, the correct size of water nanodroplet, and the correct substrate in order to control the graphene folding process.

Conclusions

We have studied the folding of a flower like graphene structure and a flake graphene structure driven by the van der Waals force between the carbon atoms and water molecules. We demonstrated that the nonbonded interactions between a graphene nanostructure and SiO_2 are strong enough to prevent the folding process. We have also demonstrated that the large contact area of a defect free system of graphene supported on a layer of IPA or HMDS over SiO_2 does not allow the graphene to fold. However, when we have a defective system over a layer of IPA supported on SiO_2 , the water–graphene interaction overcomes the graphene–substrate interaction promoting the folding process. Also when we use a hydrophobic substrate such as HMDS and the correct graphene geometry with large surface area and adequate nanodroplet size, the folding can occur. In summary, the adequate selection of substrate, graphene geometry, and nanodroplet size allows the folding and may open the possibility of a controlled fabrication of graphene-based capsules, scrolls, sandwiches, and rings.

Acknowledgment. We acknowledge financial support from the U.S. Defense Threat Reduction Agency DTRA through the U.S. Army Research Office, Project Nos. W91NF-06-1-0231 and W91NF-07-1-0199.

References and Notes

- (1) Iijima, S. Helical Microtubules of Graphitic Carbon. *Nature* **1991**, *354*, 56–58.
- (2) Novoselov, K. S.; Jiang, D.; Schedin, F.; Booth, T. J.; Khotkevich, V. V.; Morozov, S. V.; Geim, A. K. Two-Dimensional Atomic Crystals. *Proc. Natl. Acad. Sci. U.S.A.* **2005**, *102*, 10451–10453.
- (3) Novoselov, K. S.; Geim, A. K.; Morozov, S. V.; Jiang, D.; Katsnelson, M. I.; Grigorieva, I. V.; Dubonos, S. V.; Firsov, A. A. Two-Dimensional Gas of Massless Dirac Fermions in Graphene. *Nature* **2005**, *438*, 197–200.
- (4) Ebbesen, T. W.; Lezec, H. J.; Hiura, H.; Bennett, J. W.; Ghaemi, H. F.; Thio, T. Electrical Conductivity of Individual Carbon Nanotubes. *Nature* **1996**, *382*, 54–56.
- (5) Ruoff, R. S.; Lorents, D. C. Mechanical and Thermal Properties of Carbon Nanotubes. *Carbon* **1995**, *33*, 925–930.
- (6) Che, J.; Cagin, T.; Goddard, W. A., III. Thermal Conductivity of Carbon Nanotubes. *Nanotechnology* **2000**, *11*, 65–69.
- (7) Krishnan, A.; Dujardin, E.; Ebbesen, T. W.; Yianilos, P. N.; Treacy, M. M. J. Young's Modulus of Single-Walled Nanotubes. *Phys. Rev. B* **1998**, *58*, 14013.
- (8) Rangel, N. L.; Sotelo, J. C.; Seminario, J. M. Mechanism of Carbon Nanotubes Unzipping into Graphene Ribbons. *J. Chem. Phys.* **2009**, *131*, 031105.
- (9) Usui, Y.; Aoki, K.; Narita, N.; Murakami, N.; Nakamura, I.; Nakamura, K.; Ishigaki, N.; Yamazaki, H.; Horuchi, H.; Kato, H.; Taruta, S.; Kim, Y. A.; Endo, M.; Saito, N. Carbon Nanotubes with High Bone-Tissue Compatibility and Bone-Formation Acceleration Effects. *Small* **2008**, *4*, 240–246.
- (10) Du, Q. L.; Zheng, M. B.; Zhang, L. F.; Wang, Y. W.; Chen, J. H.; Xue, L. P.; Dai, W. J.; Ji, G. B.; Cao, J. M. Preparation of Functionalized Graphene Sheets by a Low-Temperature Thermal Exfoliation Approach and Their Electrochemical Supercapacitive Behaviors. *Electrochim. Acta* **2010**, *55*, 3897–3903.
- (11) Martinez, M. T.; Tseng, Y. C.; Salvador, J. P.; Marco, M. P.; Ormategui, N.; Loinaz, I.; Bokor, J. Electronic Anabolic Steroid Recognition with Carbon Nanotube Field-Effect Transistors. *Acs Nano* **2010**, *4*, 1473–1480.

- (12) Rangel, N. L.; Seminario, J. A. Graphene Terahertz Generators for Molecular Circuits and Sensors. *J. Phys. Chem. A* **2008**, *112*, 13699–13705.
- (13) Rangel, N. L.; Seminario, J. M. Vibronics and Plasmonics Based Graphene Sensors. *J. Chem. Phys.* **2010**, *132*, 125102.
- (14) He, X.; Shi, Y.; Cheng, N. M.; Pugno, H. J.; Gao, Tunable Water Channels with Carbon Nanoscrolls. *Small* **2010**, *6*, 739–744.
- (15) Xie, X.; Ju, L.; Feng, X.; Sun, Y.; Zhou, R.; Liu, K.; Fan, S.; Li, Q.; Jiang, K. Controlled Fabrication of High-Quality Carbon Nanoscrolls from Monolayer Graphene. *Nano Lett.* **2009**, *9*, 2565–2570.
- (16) Chen, Y.; Lu, J.; Gao, Z. Structural and Electronic Study of Nanoscrolls Rolled up by a Single Graphene Sheet. *J. Phys. Chem. C* **2007**, *111*, 1625–1630.
- (17) Patra, N.; Wang, B.; Krail, P. Nanodroplet Activated and Guided Folding of Graphene Nanostructures. *Nano Lett.* **2009**, *9*, 3766–3771.
- (18) Plimpton, S. Fast Parallel Algorithms for Short-Range Molecular Dynamics. *J. Comput. Phys.* **1995**, *117*, 1–19.
- (19) MacKerell, A. D.; Bashford, D.; Bellott, R. L.; Dunbrack, J. D.; Evanseck, M. J.; Field, S.; Fischer, J.; Gao, H.; Guo, S.; Ha, D.; Joseph-McCarthy, L.; Kuchnir, K.; Kuczera, F. T. K.; Lau, C.; Mattos, S.; Michnick, T.; Ngo, D. T.; Nguyen, B.; Prodhom, W. E.; Reiher, B.; Roux, M.; Schlenkrich, J. C.; Smith, R.; Stote, J.; Straub, M.; Watanabe, J.; Wiorkiewicz-Kuczera, D.; Yin, M.; Karplus. All-Atom Empirical Potential for Molecular Modeling and Dynamics Studies of Proteins. *J. Phys. Chem. B* **1998**, *102*, 3586–3616.
- (20) Cruz-Chu, E. R.; Aksimentiev, A.; Schulten, K. Water-Silica Force Field for Simulating Nanodevices. *J. Phys. Chem. B* **2006**, *110*, 21497–21508.
- (21) Lopes, P. E. M.; Murashov, V.; Tazi, M.; Demchuk, E.; MacKerell, A. D. Development of an Empirical Force Field for Silica. Application to the Quartz-Water Interface. *J. Phys. Chem. B* **2006**, *110*, 2782–2792.
- (22) Chen, I. J.; Yin, D.; MacKerell, A. D. Combined Ab Initio/Empirical Approach for Optimization of Lennard-Jones Parameters for Polar-Neutral Compounds. *J. Comput. Chem.* **2002**, *23*, 199–213.
- (23) Seminario, J. M. Calculation of Intramolecular Force Fields from Second-Derivative Tensors. *Int. J. Quantum Chem.* **1996**, *60*, 1271–1277.
- (24) Reyes, L. H.; Seminario, J. M. Determination of Precise Harmonic Force Constants for Alanine Polypeptides. *J. Mol. Struct.: THEOCHEM* **2007**, *818*, 125–129.
- (25) Bautista, E. J.; Seminario, J. M. Harmonic Force Field for Glycine Oligopeptides. *Int. J. Quantum Chem.* **2008**, *108*, 180–188.
- (26) Perdew, J. P.; Wang, Y. Accurate and Simple Analytic Representation of the Electron-Gas Correlation Energy. *Phys. Rev. B* **1992**, *45*, 13244.
- (27) Perdew, J. P.; Chevary, J. A.; Vosko, S. H.; Jackson, K. A.; Pederson, M. R.; Singh, D. J.; Fiolhais, C. Atoms, Molecules, Solids, And Surfaces: Applications of the Generalized Gradient Approximation for Exchange and Correlation. *Phys. Rev. B* **1992**, *46*, 6671.
- (28) Hariharan, P. C.; Pople, J. A. The Effect of d-Functions on Molecular Orbital Energies for Hydrocarbons. *Chem. Phys. Lett.* **1972**, *16*, 217–219.
- (29) Martínez, L.; Andrade, R.; Birgin, E. G.; Martínez, J. M. Packmol: A Package for Building Initial Configurations for Molecular Dynamics Simulations. *J. Comput. Chem.* **2009**, *30*, 2157–2164.
- (30) Shinoda, W.; Shiga, M.; Mikami, M. Rapid Estimation of Elastic Constants by Molecular Dynamics Simulation under Constant Stress. *Phys. Rev. B* **2004**, *69*, 134103.
- (31) Meyer, J. C.; Geim, A. K.; Katsnelson, M. I.; Novoselov, K. S.; Booth, T. J.; Roth, S. The Structure of Suspended Graphene Sheets. *Nature* **2007**, *446* (7131), 60–63.
- (32) Vazquez de Parga, A. L.; Calleja, F.; Borca, B.; Passeggi, M. C. G.; Hinarejos, J. J.; Guinea, F.; Miranda, R. Periodically Rippled Graphene: Growth and Spatially Resolved Electronic Structure. *Phys. Rev. Lett.* **2008**, *100* (5), 056807.
- (33) Ishigami, M.; Chen, J. H.; Cullen, W. G.; Fuhrer, M. S.; Williams, E. D. Atomic Structure of Graphene on SiO₂. *Nano Lett.* **2007**, *7* (6), 1643–1648.
- (34) Johansson, S.; Schweitz, J. A.; Lagerlof, K. P. D. Surface-Defects in Polished Silicon Studied by Cross-Sectional Transmission Electron-Microscopy. *J. Am. Ceram. Soc.* **1989**, *72*, 1136–1139.

JP108481X